

INVESTIGATING THERMAL EFFECTS IN NONLINEAR BUCKLING ANALYSIS OF MICRO BEAMS USING MODIFIED STRAIN GRADIENT THEORY*

H. MOHAMMADI** AND M. MAHZOON

Dept. of Mechanical Eng., Shiraz University, Shiraz, I. R. of Iran
Email: h_mohammadi@shirazu.ac.ir

Abstract– In this paper, thermal effects in nonlinear buckling analysis of micro beams is investigated. Modified strain gradient theory with nonlinear von-Karman strain-displacement relations and small scale parameters are used to derive the buckling behavior of micro beams. The Poisson's effect is included and its significance is demonstrated. Buckling behavior for two different cases: 1) immovable axial boundary condition 2) movable axial boundary condition, are studied and for each one the results for hinged-hinged and clamped-clamped beams are presented. The analysis shows that modified strain gradient theory leads to a higher critical buckling load in comparison with the classical and couple- stress theories. The results are verified using previous related works.

Keywords– Thermal environment, nonlinear buckling analysis, modified strain gradient theory, microbeam, nanobeam

1. INTRODUCTION

Non-classical theories play an important role in the analysis of one-dimensional micro/nano structures. Mohammadi-Alasti et al. [1] studied the mechanical behavior of a functionally graded cantilever micro-beam subjected to nonlinear electrostatic pressure and temperature changes. In addition to the Volume Fractional Rule of material, exponential function has been used for representation of continuous gradation of the material properties through micro-beam thickness. Yao and Han [2] studied the thermal effect on axially compressed buckling of a double-walled carbon nanotube. The effects of temperature change, surrounding elastic medium and van der Waals forces between the inner and outer nanotubes were taken into account. Wang et al [3] presented the thermal buckling properties of carbon nanotube with small scale effects. Based on the nonlocal continuum theory and the Timoshenko beam model, the governing equation was derived. Axial buckling characteristics of single-walled carbon nanotubes (SWCNTs) including thermal environment effect were studied by Ansari et al. [4]. It was observed that the difference between the thermal axial buckling responses of SWCNTs relevant to various boundary conditions is more prominent for higher values of nonlocal elasticity constant. Based on theory of thermal elasticity mechanics, Zhang et al. [5] developed elastic multiple column model for column buckling of MWNTs with large aspect ratios under axial compression coupling with temperature change. They concluded that the effect of temperature change on the buckling strain is dependent on the temperature changes, aspect ratios, and the buckling modes of carbon nanotubes. Zhang and Shen [6] investigated the buckling and postbuckling analysis of single-walled carbon nanotubes with (n, n) - and $(n, 0)$ -helicity, when acted upon

*Received by the editors May 15, 2013; Accepted February 3, 2014.

**Corresponding author

by the destabilizing loads of axial compression, torsion and external pressure, by using molecular dynamics simulation. Zhang and Shen [7] also studied the thermal buckling of initially compressed single-walled carbon nanotubes subjected to a uniform temperature rise by using molecular dynamics simulations. A nonlocal elastic shell model was developed to investigate the axially compressed buckling response of multi-walled carbon nanotubes considering thermal environment effect by Ansari et al. [8]. They showed that the effect of small-scale is more prominent for MWCNTs having smaller diameters and a fewer number of walls. Şimşek and Yurtcu [9] presented the static bending and buckling of a functionally graded nanobeam based on the nonlocal Timoshenko and Euler–Bernoulli beam theory. The material properties of the FG nanobeam were assumed to vary in the thickness direction. Lam et al. [10] presented new formulation of strain gradient elasticity with small scale parameters. Akgöz and Civalek [11] studied analytical solution of stability problem for axially loaded nano-sized beams based on strain gradient elasticity and modified couple stress theories. Given the importance of thermal stresses in microelectronic packaging, He et al. [12] investigated thermal characterization of epoxies. Yang and Lim [13] analyzed thermal effects on buckling of nano columns with movable axial boundary conditions and with von-Kármán nonlinearity based on nonlocal stress theory. Kong et al. [14] solved analytically the static and dynamic problems of Bernoulli–Euler beams based on strain gradient elasticity theory. Ma et al. [15] developed a microstructure-dependent Timoshenko beam model using a variational formulation. Their analysis was based on a modified couple stress theory and Hamilton's principle. The new model contained a material length scale parameter and could capture the size effect, unlike the classical Timoshenko beam theory. Analytical solutions of a general third-order plate theory that accounts for the power-law distribution of two materials through thickness and microstructure-dependent size effects were presented by Kim and Reddy [16]. The modulus of elasticity and the mass density were assumed to vary only through thickness of plate, and a single material length scale parameter of a modified couple stress theory captured the microstructure-dependent size effects. Roque et al [17] used a modified couple stress theory and a meshless method to study the bending of simply supported laminated composite beams subjected to transverse loads. The Timoshenko beam kinematics were employed to model the beam, by a modified couple stress theory. Civalek and Demir [18] developed an elastic beam model using nonlocal elasticity theory for the bending analysis of microtubules based on the Euler–Bernoulli beam theory. The size effect was taken into consideration using the Eringen's non-local elasticity theory using the method of differential quadrature method (DQM). Akgöz and Civalek [19] studied the bending analysis of micro-sized beams based on the Bernoulli-Euler theory within the modified strain gradient elasticity.

In this paper, a new nonlinear formulation considering Poisson's parameter and temperature effect is presented for micro beams. The formulation is based on modified strain gradient theory and subsequently, buckling behavior is investigated for two different boundary conditions. Results are verified using some previous related works.

2. PRELIMINARIES

In the classical linear theory of elasticity, the constitutive relations between the stress and strain is given by

$$\sigma_{ij} = \lambda e_{kk}^{el} \delta_{ij} + 2\mu e_{ij}^{el}, \quad (1)$$

where λ, μ are Lamé's coefficients and σ, e^{el} are stress and strain tensors, respectively. Solving for e^{el} we get

$$e_{ij}^{el} = \frac{1}{2\mu} \left(\sigma_{ij} - \lambda \delta_{ij} \frac{\sigma_{kk}}{3\lambda + 2\mu} \right), \quad (2)$$

Considering the effects of thermal expansion, the strain is written as

$$\varepsilon_{ij} = e_{ij}^{el} + \delta_{ij} \alpha \Delta T(x), \quad (3)$$

where α is the thermal expansion coefficient of the material and $\Delta T(x)$ is the temperature difference with respect to the free stress state. Combining Eqs. (2), (3) leads to

$$\sigma_{ij} = \lambda(\varepsilon_{kk} - 3\alpha\Delta T)\delta_{ij} + 2\mu(\varepsilon_{ij} - \delta_{ij}\alpha\Delta T) \quad (4)$$

Comparing Eq.(4) with Eq.(1) suggests that the total strain e_{ij} as defined by

$$e_{ij} = \varepsilon_{ij} - \delta_{ij}\alpha\Delta T, \quad (5)$$

can be used to find the stress, and consequently,

$$\sigma_{ij} = \lambda e_{ij} \delta_{ij} + 2\mu e_{ij}. \quad (6)$$

Lam et al. [10] presented the modified strain gradient theory that uses the stored strain energy u_m in a continuum made of a linear elastic material occupying region ϕ with infinitesimal deformations and written as

$$u_m = \frac{1}{2} \int_{\phi} \left(\sigma_{ij} \varepsilon_{ij} + p_i \gamma_i + \tau_{ijk}^{(1)} \eta_{ijk}^{(1)} + m_{ij}^s \chi_{ij}^s \right) dv, \quad (7)$$

where

$$\gamma_i = \varepsilon_{mm,i}, \quad (8)$$

$$\eta_{ijk}^{(1)} = \frac{1}{3} (e_{jk,i} + e_{ki,j} + e_{ij,k}) - \frac{1}{15} \delta_{ij} (e_{mm,k} + 2e_{mk,m}) - \frac{1}{15} [\delta_{jk} (e_{mm,i} + 2e_{mi,m}) + \delta_{ki} (e_{mm,j} + 2e_{mj,m})], \quad (9)$$

$$\chi_{ij}^s = \frac{1}{2} (\theta_{i,j} + \theta_{j,i}), \quad (10)$$

$$\theta_i = \frac{1}{2} (\text{curl}(\mathbf{u}))_i. \quad (11)$$

u_i, γ_i and θ_i represent the components of the displacement vector \mathbf{u} , the dilation gradient vector $\boldsymbol{\gamma}$, and infinitesimal rotation vector $\boldsymbol{\theta}$.

For a linear isotropic elastic material, the components of the stresses are related to the kinematic parameters by (Lam et al. [10])

$$p_i = 2\mu l_0^2 \gamma_i \quad (12)$$

$$\tau_{ijk}^{(1)} = 2\mu l_1^2 \eta_{ijk}^{(1)} \quad (13)$$

$$m_{ij}^s = 2\mu l_2^2 \chi_{ij}^s \quad (14)$$

l_0, l_1, l_2 are material length scale parameters related to dilation gradients, deviatoric stretch gradients and rotation gradients, respectively.

3. GOVERNING EQUATION

In the following formulation, the x -coordinate is taken along the length of the beam, the z -coordinate along the thickness of the beam, and the y -coordinate is taken along the width of the beam. A uniform homogeneous straight beam with length L is considered. The centroid of each section lies on the plane $z = 0$. The non-zero displacement field of an Euler-Bernoulli beam is expressed as

$$u^E = u(x) - z \frac{dw(x)}{dx}, W^E = w(x), \quad (15)$$

where u^E, W^E are the axial and transverse displacements vector and u, w represents these values in the centroid. In order to maintain consistency with uniaxial assumption we let

$$e_{22} = e_{33} = -\nu e_{11}, \quad (16)$$

where ν is the Poisson's ratio. Unlike many works, e.g.; [11, 14], here the Poisson's effect is not ignored and is included as an ad-hoc assumption in Eq. (16) and in the sequel. The nonlinear von-Karman strain is written as

$$\varepsilon_{11} = \frac{du}{dx} - z \frac{d^2w}{dx^2} + \frac{1}{2} \left(\frac{dw}{dx} \right)^2. \quad (17)$$

Substituting in Eq. (5), we get

$$e_{11} = \frac{du}{dx} - z \frac{d^2w}{dx^2} + \frac{1}{2} \left(\frac{dw}{dx} \right)^2 - \alpha \Delta T, \quad (18)$$

Using Eqs. (12-14) the non-zero components of kinematic parameters and higher order stresses are

$$\gamma_1 = (1 - 2\nu) \left(\frac{d^2u}{dx^2} - z \frac{d^3w}{dx^3} + \frac{dw}{dx} \frac{d^2w}{dx^2} - \alpha \Delta T \right), \quad \gamma_3 = -(1 - 2\nu) \frac{d^2w}{dx^2} \quad (19)$$

$$\chi_{12}^s = \chi_{21}^s = -\frac{1}{2} \frac{d^2w}{dx^2} \quad (20)$$

$$\eta_{111}^{(1)} = \frac{2}{5} (1 + \nu) \left(\frac{d^2u}{dx^2} - z \frac{d^3w}{dx^3} + \frac{dw}{dx} \frac{d^2w}{dx^2} - \alpha \frac{d(\Delta T)}{dx} \right),$$

$$\eta_{113}^{(1)} = \eta_{311}^{(1)} = \eta_{131}^{(1)} = -\frac{4}{15} (1 + \nu) \frac{d^2w}{dx^2}, \quad (21)$$

$$\eta_{122}^{(1)} = \eta_{133}^{(1)} = \eta_{212}^{(1)} = \eta_{221}^{(1)} = \eta_{313}^{(1)} = \eta_{331}^{(1)} = \frac{-1}{5} (1 + \nu) \left(\frac{d^2u}{dx^2} - z \frac{d^3w}{dx^3} + \frac{dw}{dx} \frac{d^2w}{dx^2} - \alpha \frac{d(\Delta T)}{dx} \right),$$

$$\eta_{223}^{(1)} = \eta_{232}^{(1)} = \eta_{322}^{(1)} = \frac{1}{15} (1 + \nu) \frac{d^2w}{dx^2}, \quad \eta_{333}^{(1)} = \frac{1}{5} (1 + \nu) \frac{d^2w}{dx^2}.$$

$$\sigma_{11} = E e_{11} = E \left(\frac{du}{dx} - z \frac{d^2w}{dx^2} + \frac{1}{2} \left(\frac{dw}{dx} \right)^2 - \alpha \Delta T \right), \quad (22)$$

$$p_1 = 2\mu l_0^2 (1 - 2\nu) \left(\frac{d^2u}{dx^2} - z \frac{d^3w}{dx^3} + \frac{dw}{dx} \frac{d^2w}{dx^2} - \alpha \Delta T \right), \quad p_3 = -2\mu l_0^2 (1 - 2\nu) \frac{d^2w}{dx^2} \quad (23)$$

$$m_{12}^s = m_{21}^s = -\mu l_1^2 \frac{d^2w}{dx^2}, \quad (24)$$

$$\tau_{111}^{(1)} = \mu l_1^2 \frac{4}{5} (1 + \nu) \left(\frac{d^2u}{dx^2} - z \frac{d^3w}{dx^3} + \frac{dw}{dx} \frac{d^2w}{dx^2} - \alpha \frac{d(\Delta T)}{dx} \right),$$

$$\tau_{113}^{(1)} = \tau_{311}^{(1)} = \tau_{131}^{(1)} = -\mu l_1^2 \frac{8}{15} (1 + \nu) \frac{d^2w}{dx^2}, \quad (25)$$

$$\tau_{122}^{(1)} = \tau_{133}^{(1)} = \tau_{212}^{(1)} = \tau_{221}^{(1)} = \tau_{313}^{(1)} = \tau_{331}^{(1)} = \frac{-2}{5} \mu l_1^2 (1 + \nu) \left(\frac{d^2u}{dx^2} - z \frac{d^3w}{dx^3} + \frac{dw}{dx} \frac{d^2w}{dx^2} - \alpha \frac{d(\Delta T)}{dx} \right),$$

$$\tau_{122}^{(1)} = \tau_{122}^{(1)} = \tau_{122}^{(1)} = \frac{2}{15} \mu l_1^2 (1 + \nu) \frac{d^2 w}{dx^2}, \quad \tau_{333}^{(1)} = \frac{2}{5} \mu l_1^2 (1 + \nu) \frac{d^2 w}{dx^2}.$$

Due to the residual stress, the initial axial compressive force \mathcal{N}_a is induced in the beam. The cross section area is denoted by A , area moment inertia by I and length by L . Based on Eq.(7) and considering the effect of \mathcal{N}_a the total strain energy becomes

$$\begin{aligned} \mathcal{U} &= \frac{1}{2} \int_0^L \int_A \left(E \left(\frac{du}{dx} - z \frac{d^2 w}{dx^2} + \frac{1}{2} \left(\frac{dw}{dx} \right)^2 - \alpha \Delta T \right)^2 \right. \\ &\quad + \mu \left(2l_0^2 (1 - 2\nu)^2 + l_2^2 + \frac{120}{225} l_1^2 (1 + \nu)^2 \right) \left(\frac{d^2 w}{dx^2} \right)^2 \\ &\quad + \mu \left(2l_0^2 (1 - 2\nu)^2 + \frac{4}{5} l_1^2 (1 + \nu)^2 \right) \left(\frac{d^2 u}{dx^2} - z \frac{d^3 w}{dx^3} + \frac{dw}{dx} \frac{d^2 w}{dx^2} - \alpha \frac{d(\Delta T)}{dx} \right)^2 \\ &\quad \left. - \frac{\mathcal{N}_a}{A} \left(\frac{du}{dx} - z \frac{d^2 w}{dx^2} + \frac{1}{2} \left(\frac{dw}{dx} \right)^2 - \alpha \Delta T \right) \right) dA dx \\ &= \frac{1}{2} \int_0^L \left(EA \left(\frac{du}{dx} + \frac{1}{2} \left(\frac{dw}{dx} \right)^2 - \alpha \Delta T \right)^2 - \mathcal{N}_a \left(\frac{du}{dx} + \frac{1}{2} \left(\frac{dw}{dx} \right)^2 - \alpha \Delta T \right) + k_1 \left(\frac{d^2 w}{dx^2} \right)^2 \right. \\ &\quad \left. + k_2 \left(\frac{d^3 w}{dx^3} \right)^2 + \frac{K_2}{r^2} \left(\frac{d^2 u}{dx^2} + \frac{dw}{dx} \frac{d^2 w}{dx^2} - \alpha \frac{d(\Delta T)}{dx} \right)^2 \right) dx, \end{aligned} \quad (26)$$

where

$$\begin{aligned} k_1 &= EI + \mu A \left(2l_0^2 (1 - 2\nu)^2 + l_2^2 + \frac{120}{225} l_1^2 (1 + \nu)^2 \right), \\ k_2 &= \mu I \left(2l_0^2 (1 - 2\nu)^2 + \frac{4}{5} l_1^2 (1 + \nu)^2 \right), \\ r &= \left(\frac{I}{A} \right)^{0.5}. \end{aligned} \quad (27)$$

The work done by axial compressive load p_{xx} at the end is

$$\delta \mathcal{W}_{ext} = -p_{xx} \delta u|_{x=L}. \quad (28)$$

The principle of the virtual displacement is applied

$$\delta \mathcal{W}_{ext} - \delta \mathcal{U} = 0. \quad (29)$$

Substituting Eqs. (26), (28) in Eq. (29) leads to

$$\begin{aligned} k_1 \frac{d^4 w}{dx^4} - k_2 \frac{d^6 w}{dx^6} - \frac{d}{dx} \left\{ \left(EA \left(\frac{du}{dx} + \frac{1}{2} \left(\frac{dw}{dx} \right)^2 - \alpha \Delta T \right) \right. \right. \\ \left. \left. - \frac{k_2}{r^2} \frac{d^2}{dx^2} \left(\frac{du}{dx} + \frac{1}{2} \left(\frac{dw}{dx} \right)^2 - \alpha \Delta T \right) - \mathcal{N}_a \right) \frac{dw}{dx} \right\} = 0, \end{aligned} \quad (30)$$

$$\frac{d}{dx} \left\{ -EA \left(\frac{du}{dx} + \frac{1}{2} \left(\frac{dw}{dx} \right)^2 - \alpha \Delta T \right) + \frac{k_2}{r^2} \frac{d^2}{dx^2} \left(\frac{du}{dx} + \frac{1}{2} \left(\frac{dw}{dx} \right)^2 - \alpha \Delta T \right) + \mathcal{N}_a \right\} = 0, \quad (31)$$

$$\begin{aligned} \left\{ -k_1 \frac{d^3 w}{dx^3} + k_2 \frac{d^5 w}{dx^5} + \frac{dw}{dx} \left(EA \left(\frac{du}{dx} + \frac{1}{2} \left(\frac{dw}{dx} \right)^2 - \alpha \Delta T \right) \right. \right. \\ \left. \left. - \frac{k_2}{r^2} \frac{d^2}{dx^2} \left(\frac{du}{dx} + \frac{1}{2} \left(\frac{dw}{dx} \right)^2 - \alpha \Delta T \right) - \mathcal{N}_a \right) \right\} \delta w|_{x=L} = 0, \end{aligned} \quad (32)$$

$$\left\{ k_1 \frac{d^2 w}{dx^2} - k_2 \frac{d^4 w}{dx^4} + \frac{k_2}{r^2} \frac{dw}{dx} \frac{d}{dx} \left(\frac{du}{dx} + \frac{1}{2} \left(\frac{dw}{dx} \right)^2 - \alpha \Delta T \right) \right\} \delta \frac{dw}{dx}|_{x=0} = 0, \quad (33)$$

$$\left\{K_2 \frac{d^3 w}{dx^3}\right\} \delta \frac{d^2 w}{dx^2} \Big|_{x=0}^{x=L} = 0, \quad (34)$$

$$\left\{EA \left(\frac{du}{dx} + \frac{1}{2} \left(\frac{dw}{dx}\right)^2 - \alpha \Delta T\right) - \frac{K_2}{r^2} \frac{d^2}{dx^2} \left(\frac{du}{dx} + \frac{1}{2} \left(\frac{dw}{dx}\right)^2 - \alpha \Delta T\right) - N_a + p_{xx}\right\} \delta u \Big|_{x=0}^{x=L} = 0, \quad (35)$$

$$\left\{\frac{K_2}{r^2} \frac{d}{dx} \left(\frac{du}{dx} + \frac{1}{2} \left(\frac{dw}{dx}\right)^2 - \alpha \Delta T\right)\right\} \delta \frac{du}{dx} \Big|_{x=0}^{x=L} = 0. \quad (36)$$

Equations (30) and (31) describe the governing equations of the nonlinear Euler-Bernoulli beam, while Eqs. (32-36) represent the boundary conditions. Equations (32), (33), (35) denote the classical boundary conditions and Eqs.(34) and (36) show the non-classical boundary conditions resulting from higher stresses. If Poisson's effect, temperature differences and nonlinear terms are neglected, the Eqs.(30-36) reduce to those presented by Akgöz and Civalek[11]. Equations (27, 28, 30-36) indicate that if $l_0 = l_1 = 0$ (like modified couple stress theory [20-28], classic theory) the Poisson's effect can be neglected, but if $l_0 \neq 0, l_1 \neq 0$ (like modified strain gradient theory) the Poisson's effect must be considered. Introducing the following variables, non-dimensional form of Eqs. (27-33) are derived

$$W = \frac{w}{L}, U = \frac{u}{L}, X = \frac{x}{L}, b_0 = \frac{r}{L}, N_a = \frac{N_a L^2}{EI}, K_1 = \frac{k_1}{EI}, K_2 = \frac{k_2}{EIL^2}, P_{xx} = \frac{p_{xx} L^2}{EI},$$

$$\Delta T(X, t) = \Delta T(XL, t), K_1 = 1 + \frac{\mu}{b_0^2 E} \left(2L_0^2(1 - 2\nu)^2 + L_2^2 + \frac{120}{225} L_1^2(1 + \nu)^2\right), \quad (37)$$

$$K_2 = \frac{\mu}{E} \left(2L_0^2(1 - 2\nu)^2 + \frac{4}{5} L_1^2(1 + \nu)^2\right), l_0 = \frac{L_0}{L}, l_1 = \frac{L_1}{L}, l_2 = \frac{L_2}{L},$$

$$K_1 \frac{d^4 W}{dX^4} - K_2 \frac{d^6 W}{dX^6} - \frac{d}{dX} \left\{ \left(\frac{1}{b_0^2} \left(\frac{dU}{dX} + \frac{1}{2} \left(\frac{dW}{dX} \right)^2 - \alpha \Delta T \right) \right) \right. \\ \left. - \frac{K_2}{b_0^2} \frac{d^2}{dX^2} \left(\frac{dU}{dX} + \frac{1}{2} \left(\frac{dW}{dX} \right)^2 - \alpha \Delta T \right) - N_a \right\} \frac{dW}{dX} = 0, \quad (38)$$

$$\frac{d}{dX} \left\{ -\frac{1}{b_0^2} \left(\frac{dU}{dX} + \frac{1}{2} \left(\frac{dW}{dX} \right)^2 - \alpha \Delta T \right) + \frac{K_2}{b_0^2} \frac{d^2}{dX^2} \left(\frac{dU}{dX} + \frac{1}{2} \left(\frac{dW}{dX} \right)^2 - \alpha \Delta T \right) + N_a \right\} = 0, \quad (39)$$

$$\left\{ -K_1 \frac{d^3 W}{dX^3} + K_2 \frac{d^5 W}{dX^5} + \frac{dW}{dX} \left(\frac{1}{b_0^2} \left(\frac{dU}{dX} + \frac{1}{2} \left(\frac{dW}{dX} \right)^2 - \alpha \Delta T \right) \right. \right. \\ \left. \left. - \frac{K_2}{b_0^2} \frac{d^2}{dX^2} \left(\frac{dU}{dX} + \frac{1}{2} \left(\frac{dW}{dX} \right)^2 - \alpha \Delta T \right) - N_a \right) \right\} \delta W \Big|_{X=0}^{X=1} = 0, \quad (40)$$

$$\left\{ K_1 \frac{d^2 W}{dX^2} - K_2 \frac{d^4 W}{dX^4} + \frac{K_2}{b_0^2} \frac{dW}{dX} \frac{d}{dX} \left(\frac{dU}{dX} + \frac{1}{2} \left(\frac{dW}{dX} \right)^2 - \alpha \Delta T \right) \right\} \delta \frac{dW}{dX} \Big|_{X=0}^{X=1} = 0, \quad (41)$$

$$\left\{ K_2 \frac{d^3 W}{dX^3} \right\} \delta \frac{d^2 W}{dX^2} \Big|_{X=0}^{X=1} = 0, \quad (42)$$

$$\left\{ \frac{1}{b_0^2} \left(\frac{dU}{dX} + \frac{1}{2} \left(\frac{dW}{dX} \right)^2 - \alpha \Delta T \right) - \frac{K_2}{b_0^2} \frac{d^2}{dX^2} \left(\frac{dU}{dX} + \frac{1}{2} \left(\frac{dW}{dX} \right)^2 - \alpha \Delta T \right) - N_a + P_{xx} \right\} \delta U \Big|_{X=0}^{X=1} = 0, \quad (43)$$

$$\left\{ \frac{K_2}{b_0^2} \frac{d}{dX} \left(\frac{dU}{dX} + \frac{1}{2} \left(\frac{dW}{dX} \right)^2 - \alpha \Delta T \right) \right\} \delta \frac{dU}{dX} \Big|_{X=0}^{X=1} = 0. \quad (44)$$

4. RESULTS

The temperature effects on the buckling of nonlinear micro beams are studied for immovable and movable boundaries (Fig. 1). For each case two boundary conditions, hinged-hinged and clamped-clamped are

investigated. Results are verified using previous works. It must be noted that initial axial compressive force N_a is constant.

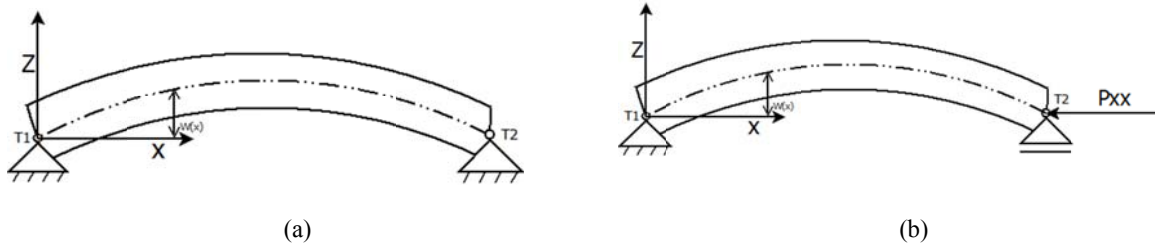


Fig. 1. Schematic diagram of microbeam: a) immovable axial boundary condition
b) movable axial boundary condition

a) Immovable axial boundary condition

In this state the general boundary conditions from Eqs. (40), (43), (44) become

$$W(0) = W(1) = 0, \tag{45}$$

$$U(0) = U(1) = 0, \tag{46}$$

$$(U' + \frac{1}{2}W'^2 - \alpha\Delta T)' \Big|_{X=0} = (U' + \frac{1}{2}W'^2 - \alpha\Delta T)' \Big|_{X=1} = 0, \tag{47}$$

where ' represents derivative with respect to X . According to Eq. (39)

$$\frac{1}{b_0^2} (U' + \frac{1}{2}W'^2 - \alpha\Delta T) - N_a = C_{11} \sinh\left(\frac{1}{\sqrt{K_2}}X\right) + C_{12} \cosh\left(\frac{1}{\sqrt{K_2}}X\right) + C_{13}, (K_2 \neq 0) \tag{48}$$

Applying boundary conditions of Eq. (47) we get

$$C_{11} = 0, C_{12} = 0, \tag{49}$$

So,

$$\tilde{N} = -\frac{1}{b_0^2} (U' + \frac{1}{2}W'^2 - \alpha\Delta T) + N_a, \tag{50}$$

where \tilde{N} is independent of X . Note that if $K_2 = 0$, Eq.(50) results directly from Eq.(39). Taking the derivative of Eq.(50) relative to X and rearranging it

$$U'' = -\left(\frac{1}{2}W'^2 - \alpha\Delta T\right)', \tag{51}$$

Taking two time integration with respect to X

$$U = -\int_0^X \left(\frac{1}{2}W'^2 - \alpha\Delta T\right) dX + C_{21}X + C_{22}, \tag{52}$$

applying Eq. (45)

$$C_{21} = \int_0^1 \left(\frac{1}{2}W'^2 - \alpha\Delta T\right) dX, C_{22} = 0, \tag{53}$$

so

$$\tilde{N} = -\frac{1}{b_0^2} \int_0^1 \left(\frac{1}{2}W'^2 - \alpha\Delta T\right) dX + N_a. \tag{54}$$

The axial force due to thermal effect is defined by

$$N_T = \frac{1}{b_0^2} \int_0^1 \alpha\Delta T dX. \tag{55}$$

If temperature distribution is assumed to be linear, N_T becomes

$$N_T = \frac{\alpha}{b_0^2} \frac{T_2 - T_1}{2} \quad (56)$$

where T_2 , T_1 are temperatures at the micro beam ends and it is assumed that $T_2 \geq T_1$.

Equation (50) is substituted in Eq. (38) to get

$$K_2 \frac{d^6 W}{dX^6} - K_1 \frac{d^4 W}{dX^4} - \tilde{N} \frac{d^2 W}{dX^2} = 0. \quad (57)$$

Solution of Eq. (57) is

$$W = C_1 \sin(\lambda_1 X) + C_2 \cos(\lambda_1 X) + C_3 \sinh(\lambda_2 X) + C_4 \cosh(\lambda_2 X) + C_5 X + C_6, \quad (58)$$

where

$$\lambda_1 = \left(\frac{-K_1 + \sqrt{K_1^2 + 4K_2 \tilde{N}}}{2K_2} \right)^{0.5}, \quad \lambda_2 = \left(\frac{K_1 + \sqrt{K_1^2 + 4K_2 \tilde{N}}}{2K_2} \right)^{0.5}, \quad (59)$$

and it is assumed that

$$K_1^2 + 4K_2 \tilde{N} \geq 0 \quad (60)$$

1. Buckling of hinged-hinged beam with immovable axial boundaries

Equations (41) and (42) imply the boundary conditions

$$\left. \frac{d^4 W}{dX^4} \right|_{X=0} = \left. \frac{d^4 W}{dX^4} \right|_{X=1} = 0, \quad (61)$$

$$W''(0) = W''(1) = 0. \quad (62)$$

With these boundary conditions the non-trivial solution is

$$W = C_1 \sin(n\pi X), \quad (n = 1, 2, \dots), \quad (63)$$

$$\tilde{N} = K_1 (n\pi)^2 + K_2 (n\pi)^4, \quad (64)$$

which satisfies Eq.(60), so the critical buckling load of modified strain gradient theory becomes

$$\begin{aligned} \tilde{N}_{cr}^{MS} &= (N_T + N_a)_{cr}^{MS} = K_1 (n\pi)^2 + K_2 (n\pi)^4 \\ &= \left(1 + \frac{\mu}{b_0^2 E} \left(2L_0^2 (1 - 2\nu)^2 + L_2^2 + \frac{120}{225} L_1^2 (1 + \nu)^2 \right) \right) (n\pi)^2 \\ &\quad + \frac{\mu}{E} \left(2L_0^2 (1 - 2\nu)^2 + \frac{4}{5} L_1^2 (1 + \nu)^2 \right) (n\pi)^4. \end{aligned} \quad (65)$$

If temperature difference and Poisson's effects are neglected, Eq. (65) reduces to the results presented by Akgoz and Civalek [11]. For numerical illustration it is assumed that the beam is made of epoxy with $E = 1.44 \text{ Gpa}$, $\nu = .38$, $\alpha = 22.4 \mu/\text{°C}$ [11, 12]. If not stated, additional material length scale parameters are set to $L_0 = L_1 = L_2 = 17.6 \mu\text{m}$ for MSGT and $L_0 = L_1 = 0, L_2 = 17.6 \mu\text{m}$ for MCST. Figure 2 shows the critical buckling load for various ratios of length to thickness based on the modified strain gradient theory (MSGT) for $\nu = 0$ and $\nu = 0.38$. The cross section is the same as [11]: a rectangle with thickness h and width $b = 2h$ and length $L = 20h$. The results are compared with Akgöz, Civalek [11] and show exact consistency with MSGT($\nu = 0$). Figure 2 shows that if the Poisson's ratio is not zero, buckling load decreases. By increasing the ratio of length to thickness the size effect decreases and there is no significant difference between the two cases.

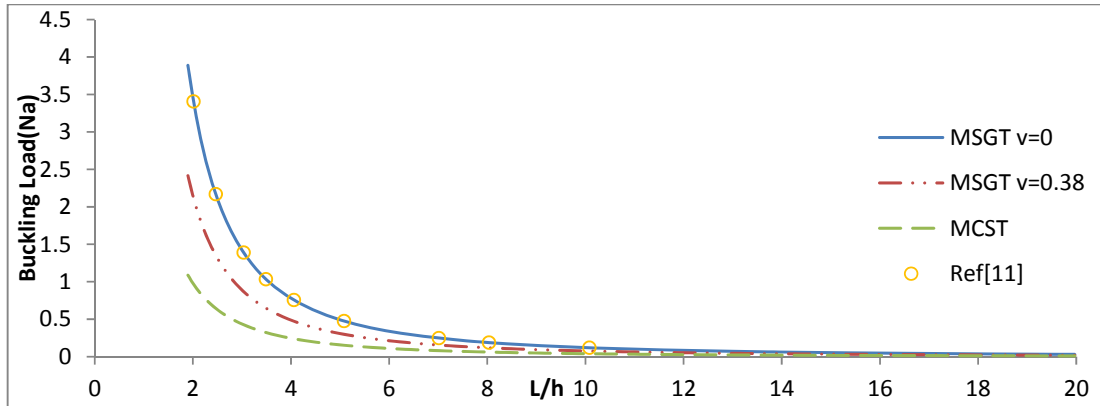


Fig. 2. Critical buckling load N_a (μN) for simply supported beam for various theories ($h = 17.6 \mu m$)

For the special case $L_0 = L_1 = 0$, buckling load of modified couple stress theory (MCST) is computed while $L_0 = L_1 = L_2 = 0$ leads to the classical Euler-Bernoulli buckling load

$$\tilde{N}_{cr}^{MC} = \left(1 + \frac{\mu}{E} L_2^2\right) (n\pi)^2, \tag{66}$$

$$\tilde{N}_{cr}^{cl} = \frac{N_{cr}^{cl} L^2}{EI} = (n\pi)^2. \tag{67}$$

Comparing Eqs. (65-68) we conclude that

$$\tilde{N}_{cr}^{MS} > \tilde{N}_{cr}^{MC} > \tilde{N}_{cr}^{cl}. \tag{68}$$

In the case $N_a = 0$ the critical temperature difference becomes

$$(T_2 - T_1)_{cr}^{MS} = \frac{2b_0^2}{\alpha} \{K_1(n\pi)^2 + K_2(n\pi)^4\} \tag{69}$$

2. Buckling of clamped-clamped beam with immovable axial boundaries

Equations (41) and (42) imply the boundary conditions

$$\left. \frac{d^3 W}{dX^3} \right|_{X=0} = \left. \frac{d^3 W}{dX^3} \right|_{X=1} = 0, \tag{70}$$

$$W'(0) = W'(1) = 0. \tag{71}$$

Applying Eqs. (45), (70), (71) and (58) we get the non-trivial solution as

$$W = C_2(\cos(2n\pi X) - 1), \quad (n = 1, 2, \dots) \tag{72}$$

$$\tilde{N} = K_1(2n\pi)^2 + K_2(2n\pi)^4 \tag{73}$$

So the critical buckling load of modified strain gradient theory becomes

$$\begin{aligned} \tilde{N}_{cr}^{MS} &= (N_T + N_a)_{cr}^{MS} = K_1(2n\pi)^2 + K_2(2n\pi)^4 \\ &= \left(1 + \frac{\mu}{b_0^2 E} \left(2L_0^2(1 - 2\nu)^2 + L_2^2 + \frac{120}{225} L_1^2(1 + \nu)^2\right)\right) (2n\pi)^2 \\ &\quad + \frac{\mu}{E} \left(2L_0^2(1 - 2\nu)^2 + \frac{4}{5} L_1^2(1 + \nu)^2\right) (2n\pi)^4. \end{aligned} \tag{74}$$

For the special case $L_0 = L_1 = 0$ buckling load of modified couple stress theory is computed while $L_0 = L_1 = L_2 = 0$ leads to the classical Euler-Bernoulli buckling load

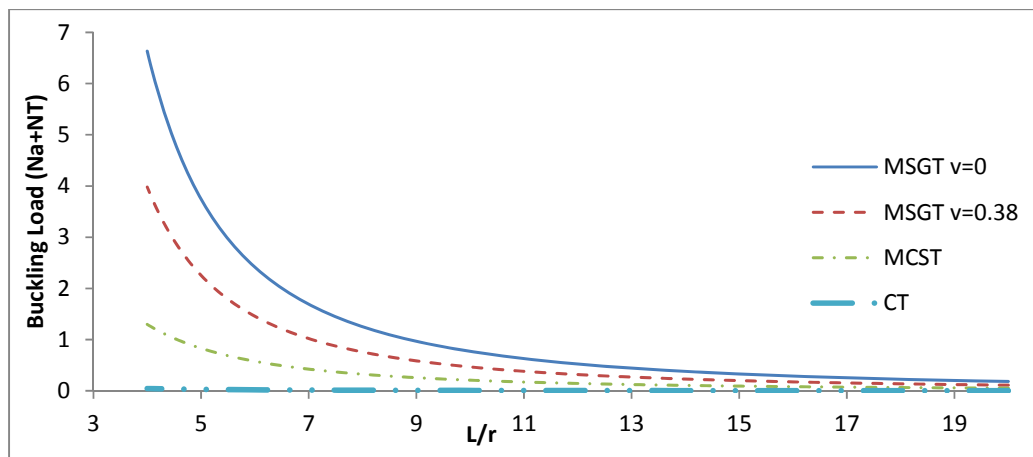
$$\tilde{N}_{cr}^{MC} = \left(1 + \frac{\mu}{E} L_2^2\right) (2n\pi)^2, \tag{75}$$

$$\tilde{N}_{cr}^{cl} = \frac{N_{cr}^{cl} L^2}{EI} = (2n\pi)^2. \quad (76)$$

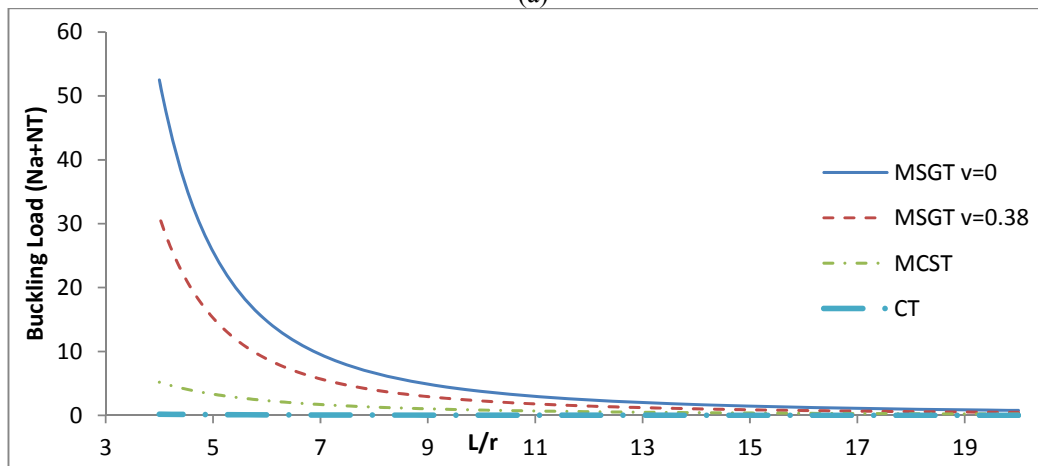
In the case $N_a = 0$ the critical temperature difference becomes

$$(T_2 - T_1)_{cr}^{MS} = \frac{2b_0^2}{\alpha} \{K_1(2n\pi)^2 + K_2(2n\pi)^4\} \quad (77)$$

In the following numerical examples circular cross sections with radius of gyration r are considered. Figures 3a and 3b show variation of critical buckling load N_{cr} with respect to L/r based on four different approaches (MSGT($\nu = 0$), MSGT($\nu = 0.38$), MCST, CT) for hinged-hinged and clamped-clamped boundary conditions. As the figures indicate, for lower values of L/r different results are obtained for buckling load, while for higher L/r results for all approaches converge. MSGT predicts the highest critical loads when Poisson's effect is ignored and MSCT shows lower buckling load as compared to MSGT. CT results are significantly different as compared to MSGT and MSCT because of the importance of additional material length scale parameters. As expected, clamped-clamped boundary conditions predict larger values for the buckling load. Figure 4 shows that for large L/r thermal buckling can occur in a range of 100 °C temperature difference, which indicates when ratio of length to radius of gyration is high, the microbeam is very sensitive to thermal buckling.



(a)



(b)

Fig. 3. Critical buckling load $N_a + NT$ (μN) for a) hinged-hinged b) clamped-clamped beam for various theories ($L_2 = 17.6 \mu m$, $r = 2 \mu m$)

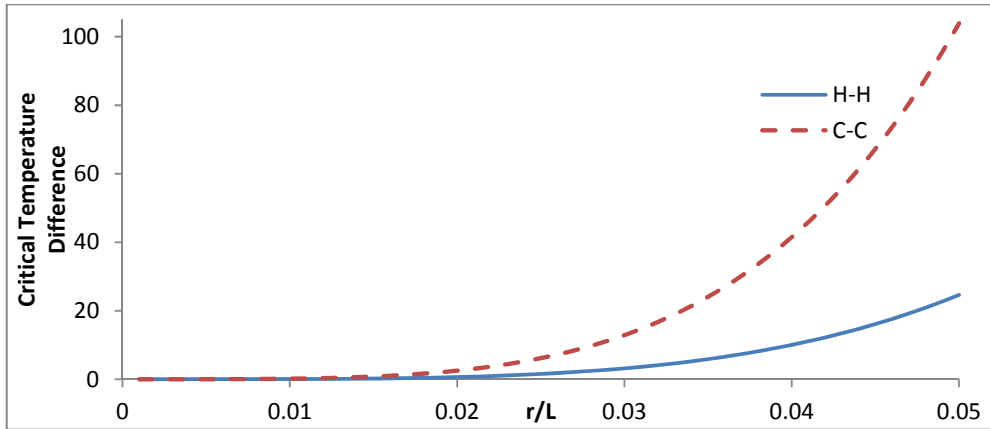
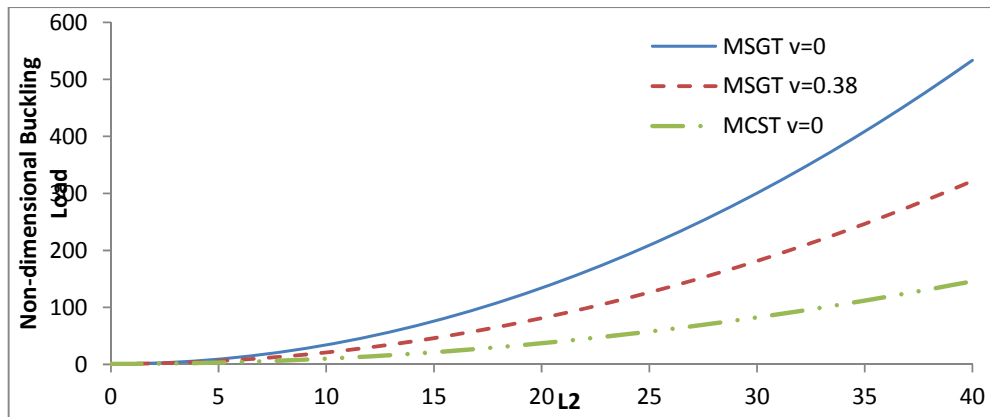
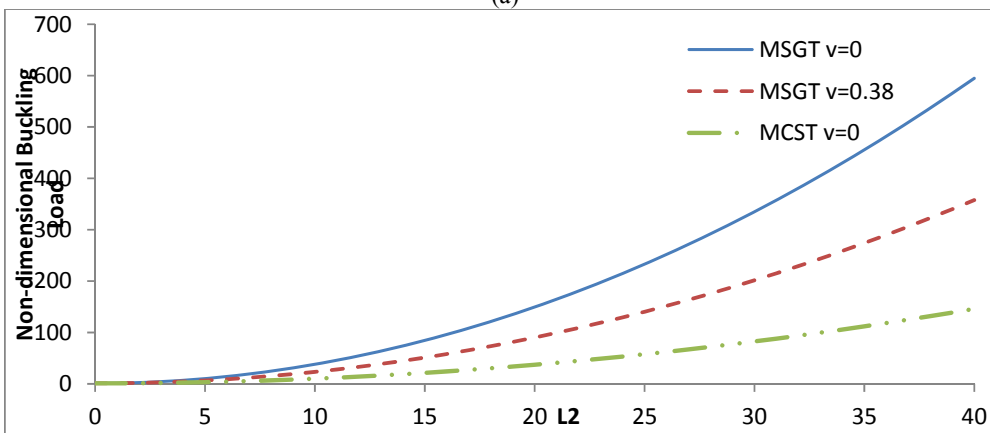


Fig. 4. Critical Temperature Difference (°C) hinged-hinged(H-H), clamped-clamped(C-C) beam by MSGT ($L_2 = 17.6 \mu m, r = 2 \mu m$)

Figure 5 shows the ratio of buckling load to Euler Buckling load versus small scale parameter using various approaches (MSGT($v = 0$), MSGT($v = 0.38$), MCST) for hinged-hinged and clamped-clamped boundary conditions. For MSGT it is assumed that $L_0 = L_1 = L_2$. MSGT with $v = 0$ predicts the highest buckling load and as the scale parameters increase the discrepancy in the buckling load as predicted by various approaches also increases.



(a)



(b)

Fig. 5. Non-dimensional buckling load a) hinged-hinged b)clamped-clamped by various theories ($L = 28 \mu m, r = 2 \mu m$)

b) Movable axial boundary conditions

In this state the general boundary conditions from Eqs.(40) , (43), (44) become

$$W(0) = W(1) = 0, \quad (78)$$

$$U(0) = 0, \quad (79-a)$$

$$\left\{ \frac{1}{b_0^2} \left(U' + \frac{1}{2} W'^2 - \alpha \Delta T \right) - \frac{K_2}{b_0^2} \left(U' + \frac{1}{2} W'^2 - \alpha \Delta T \right)'' - N_a + P_{xx} \right\} \Big|_{x=1} = 0, \quad (79-b)$$

$$\left(U' + \frac{1}{2} W'^2 - \alpha \Delta T \right) \Big|_{x=0} = 0, \quad (80-a)$$

$$U'(1) = 0, \quad (80-b)$$

According to Eq. (42)

$$\frac{1}{b_0^2} \left(U' + \frac{1}{2} W'^2 - \alpha \Delta T \right) - N_a = C_{31} \sinh \left(\frac{1}{\sqrt{K_2}} X \right) + C_{32} \cosh \left(\frac{1}{\sqrt{K_2}} X \right) + C_{33}, (K_2 \neq 0) \quad (81)$$

Applying boundary conditions of Eqs. (79-b), (80-a)

$$C_{31} = 0, C_{33} = -P_{xx}, \quad (82)$$

so

$$\tilde{N} = -\frac{1}{b_0^2} \left(U' + \frac{1}{2} W'^2 - \alpha \Delta T \right) + \frac{K_2}{b_0^2} \left(U' + \frac{1}{2} W'^2 - \alpha \Delta T \right)'' + \quad (83-a)$$

$$N_a = N_T + N_a + N_{xx} = P_{xx},$$

where \tilde{N} is independent of X and N_{xx} is the compression load induced by the presence of axial strain in the microbeam.

If $K_2 = 0$ instead of Eqs.(81-83) we have

$$\tilde{N} = -\frac{1}{b_0^2} \left(U' + \frac{1}{2} W'^2 - \alpha \Delta T \right) + N_a = -C_{33} = P_{xx}, \quad (83-b)$$

Equations (83) and (50) indicate that the presence of N_{xx} is the result of small size parameters and movable axial boundary condition. If Eq. (83) is substituted in the governing Eq. (38), Eq. (56) results that its solution is in the form of Eq. (58).

1. Buckling of hinged-hinged movable axial boundaries

Equations (41), (42) imply the same boundary conditions as Eqs. (61), (62). Boundary Eqs. (45), (61), (62) give the non-trivial solution as Eq. (63). So the critical buckling load of modified strain gradient theory becomes

$$\begin{aligned} N_{cr}^{MS} &= (N_T + N_a + N_{xx})_{cr}^{MS} = (P_{xx})_{cr}^{MS} = K_1(n\pi)^2 + K_2(n\pi)^4 \\ &= \left(1 + \frac{\mu}{b_0^2 E} \left(2L_0^2(1-2\nu)^2 + L_2^2 + \frac{120}{225} L_1^2(1+\nu)^2 \right) \right) (n\pi)^2 \\ &\quad + \frac{\mu}{E} \left(2L_0^2(1-2\nu)^2 + \frac{4}{5} L_1^2(1+\nu)^2 \right) (n\pi)^4, \end{aligned} \quad (84)$$

where n denotes the buckling mode. The instability solutions for a hinged-hinged micro beam with movable boundary condition is

$$\begin{aligned} (N_{xx})_{cr}^{MS} &= (P_{xx})_{cr}^{MS} - (N_T + N_a) = K_1(n\pi)^2 + K_2(n\pi)^4 - (N_T + N_a) \\ &= \left(1 + \frac{\mu}{b_0^2 E} \left(2L_0^2(1-2\nu)^2 + L_2^2 + \frac{120}{225} L_1^2(1+\nu)^2 \right) \right) (n\pi)^2 \end{aligned} \quad (85)$$

$$+ \frac{\mu}{E} \left(2L_0^2(1-2v)^2 + \frac{4}{5}L_1^2(1+v)^2 \right) (n\pi)^4 - \frac{\alpha}{b_0^2} \frac{T_2-T_1}{2} - N_a.$$

Comparing Eq.(65) with (85) we see that $(N_{xx})_{cr}^{MS}$ is zero for immovable boundary condition. When $L_0 = L_1 = L_2 = 0$ and $N_a = 0$ the results are the same as for the classical case presented by Yang and Lim[13].

$$(N_{xx})_{cr}^{CL} = (n\pi)^2 - \frac{\alpha}{b_0^2} \frac{T_2-T_1}{2}. \quad (86)$$

Special case with $L_0 = L_1 = 0$ presents the modified couple stress result

$$(N_{xx})_{cr}^{MS} = \left(1 + \frac{\mu}{b_0^2 E} L_2^2 \right) (n\pi)^2 - \frac{\alpha}{b_0^2} \frac{T_2-T_1}{2}. \quad (87)$$

Comparing Eqs. (85-87), we conclude

$$(N_{xx})_{cr}^{MS} > (N_{xx})_{cr}^{MC} > (N_{xx})_{cr}^{CL}. \quad (88)$$

In extreme case $(N_{xx})_{cr}^{SG} = 0$ the critical temperature difference is obtained

$$(T_2 - T_1)_{cr}^{MS} = \frac{2b_0^2}{\alpha} \{ K_1(n\pi)^2 + K_2(n\pi)^4 - N_a \}. \quad (89)$$

Increasing $(T_2 - T_1)$ decreases the compressive load induced by the presence of axial strain until $(T_2 - T_1)$ reaches $(T_2 - T_1)_{cr}$ where all compressive strain in the microbeam is due to thermal strain. Investigating Eq. (81) shows that P_{xx} is the buckling load and in contrast to immovable axial boundary conditions N_T , N_a would not yield buckling in immovable axial boundary conditions, the induced compressive axial load N_{xx} can be changed. This means that the thermal effect in movable and immovable axial boundary conditions are completely different and as discussed, critical temperature difference for the two cases has its own meaning.

2. Buckling of clamped-clamped movable axial boundaries

Eqs.(41) and (42) imply the boundary conditions as Eqs.(70), (71). Boundary Eqs.(45), (70), (71) lead to the non-trivial solution as Eq.(72). So the critical buckling load of modified strain gradient theory becomes

$$\begin{aligned} N_{cr}^{MS} &= (N_T + N_a + N_{xx})_{cr}^{MS} = (P_{xx})_{cr}^{MS} = K_1(2n\pi)^2 + K_2(2n\pi)^4 \\ &= \left(1 + \frac{\mu}{b_0^2 E} \left(2L_0^2(1-2v)^2 + L_2^2 + \frac{120}{225}L_1^2(1+v)^2 \right) \right) (2n\pi)^2 \\ &\quad + \frac{\mu}{E} \left(2L_0^2(1-2v)^2 + \frac{4}{5}L_1^2(1+v)^2 \right) (2n\pi)^4, \end{aligned} \quad (90)$$

where n denotes the mode of buckling. The instability solutions for a clamped-clamped micro beam with movable boundary condition is

$$\begin{aligned} (N_{xx})_{cr}^{MS} &= (P_{xx})_{cr}^{MS} - (N_T + N_a) = K_1(2n\pi)^2 + K_2(2n\pi)^4 - (N_T + N_a) \\ &= \left(1 + \frac{\mu}{b_0^2 E} \left(2L_0^2(1-2v)^2 + L_2^2 + \frac{120}{225}L_1^2(1+v)^2 \right) \right) (2n\pi)^2 \\ &\quad + \frac{\mu}{E} \left(2L_0^2(1-2v)^2 + \frac{4}{5}L_1^2(1+v)^2 \right) (2n\pi)^4 - \frac{\alpha}{b_0^2} \frac{T_2-T_1}{2} - N_a. \end{aligned} \quad (91)$$

EquationS (90) and (91) show that $(N_{xx})_{cr}^{MS}$ is zero for immovable boundary condition. When $L_0 = L_1 = L_2 = 0$ and $N_a = 0$ the results are the same as for the classical theory presented by Yang and Lim[13].

$$(N_{xx})_{cr}^{CL} = (2n\pi)^2 - \frac{\alpha}{b_0^2} \frac{T_2 - T_1}{2}. \tag{92}$$

Special case with $L_0 = L_1 = 0$ presents the modified couple stress result

$$(N_{xx})_{cr}^{MC} = \left(1 + \frac{\mu}{b_0^2 E} L_2^2\right) (n\pi)^2 - \frac{\alpha}{b_0^2} \frac{T_2 - T_1}{2}. \tag{93}$$

In the limiting case $(N_{xx})_{cr}^{MS} = 0$, the critical temperature difference is obtained

$$(T_2 - T_1)_{cr}^{MS} = \frac{2b_0^2}{\alpha} \{K_1(2n\pi)^2 + K_2(2n\pi)^4 - N_a\}. \tag{94}$$

In the following numerical examples, $N_a = 0$. Figure 6 shows the effect of temperature difference on the non- dimensional buckling load $(N_{xx})_{cr} / (P_{xx})_{cr}$. Larger temperature difference for larger values of L/r decreases induced axial compressive load. It is seen that for small values of L/r , regardless of the value of ΔT , all of the compressive load is due to N_{xx} . For zero ΔT , $(N_{xx})_{cr} = (P_{xx})_{cr}$ and we get a straight horizontal curve in Fig. 6. Thermal effect for hinged-hinged microbeam is larger than clamped-clamped one.

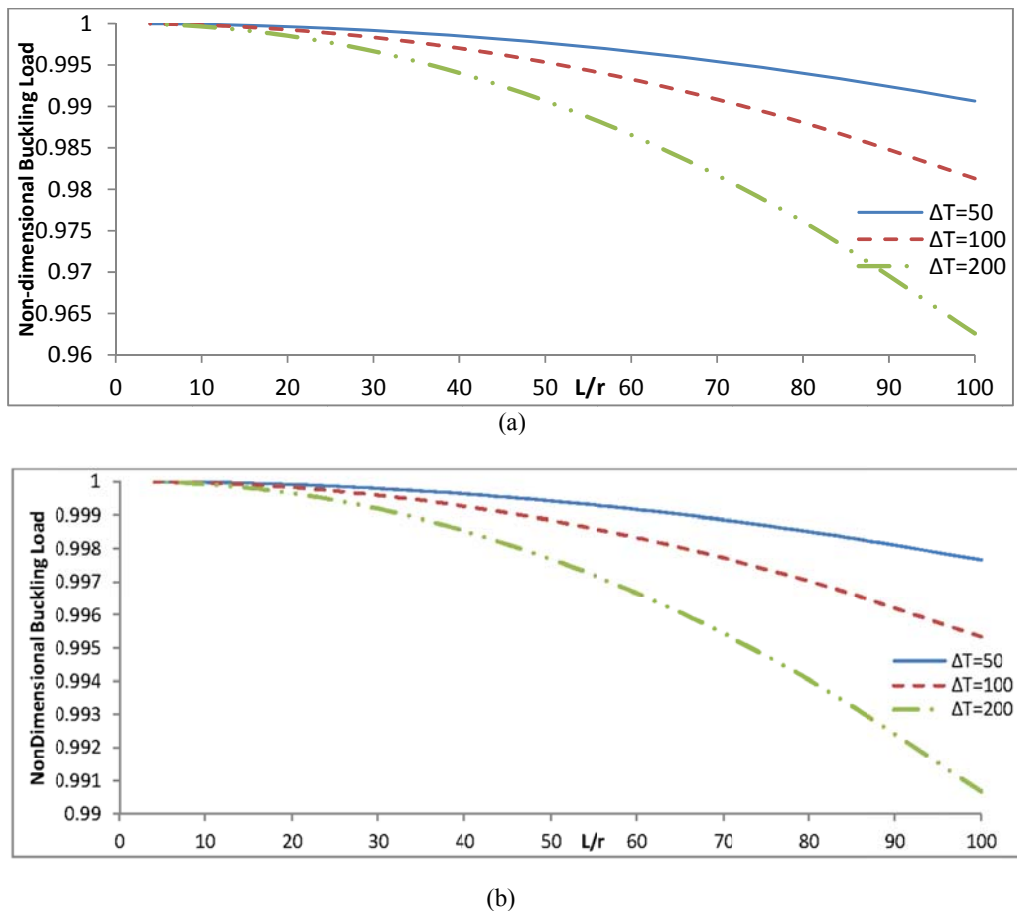
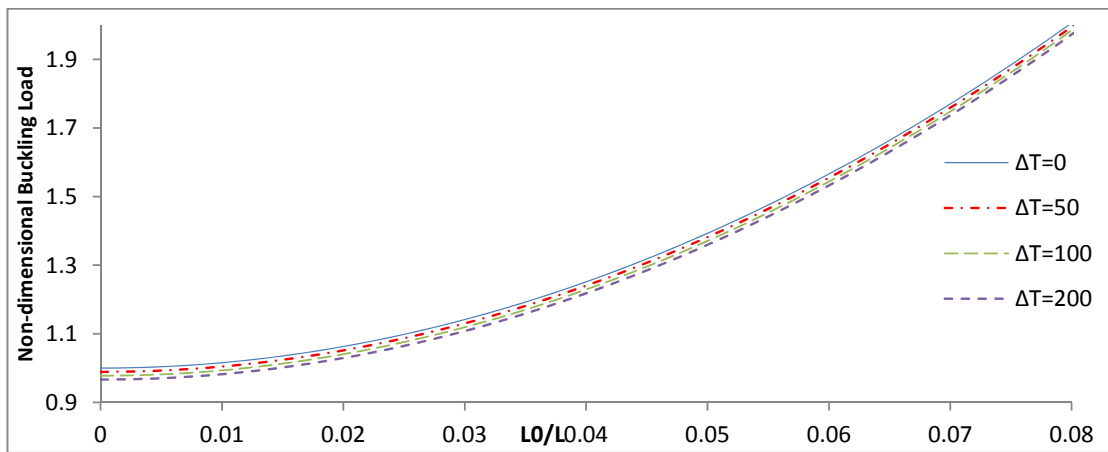


Fig. 6. Effect of temperature difference on non-dimensional buckling load a) hinged-hinged b) clamped-clamped by various theories ($L_2 = 17.6 \mu m, r = 2 \mu m$)

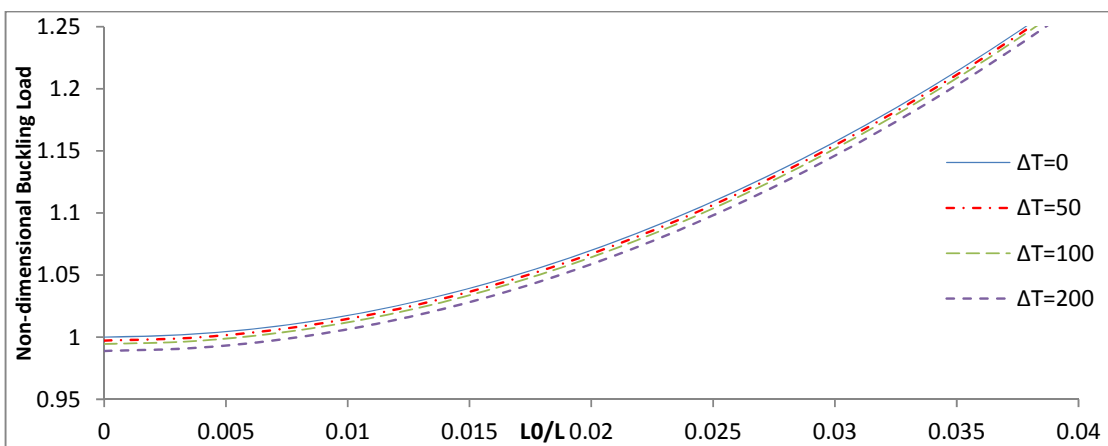
Figure 7 indicates that $(N_{xx})_{cr}^{MS}/(N_{xx})_{cr}^{CL}$ increases with increasing small scale parameters. It is observed that increasing temperature difference decreases the ratio between two critical load computed by two theories: $(N_{xx})_{cr}^{MS}, (N_{xx})_{cr}^{CL}$.

Studying the effects of geometrical shape plays an important role in investigating the buckling behavior of both macro/micro structures [16, 28-31]. Figure 8 shows ratio of the critical temperature difference $(T_2 - T_1)_{cr}^{MS}/(T_2 - T_1)_{cr}^{CT}$ vs. r/L . It is seen that this ratio and stiffness of microbeam increases with increasing r/L and increasing small scale parameters. For small values of r/L there is no significant difference between MSGT, MCST, CT.

Figure 9 shows the variation of thermal buckling load vs. small scale parameter. It is seen that by increasing the small scale parameter the thermal buckling load increases. For higher modes the rate of increasing of thermal buckling load with small scale parameter is higher. This was expected because it is generally known that the small scale parameter effect is more significant for higher modes.



(a)



(b)

Fig. 7. Effect of temperature difference on non-dimensional buckling load for various additional material parameters a) hinged-hinged b) clamped-clamped by various theories ($L = 28 \mu m, r = 2 \mu m$)

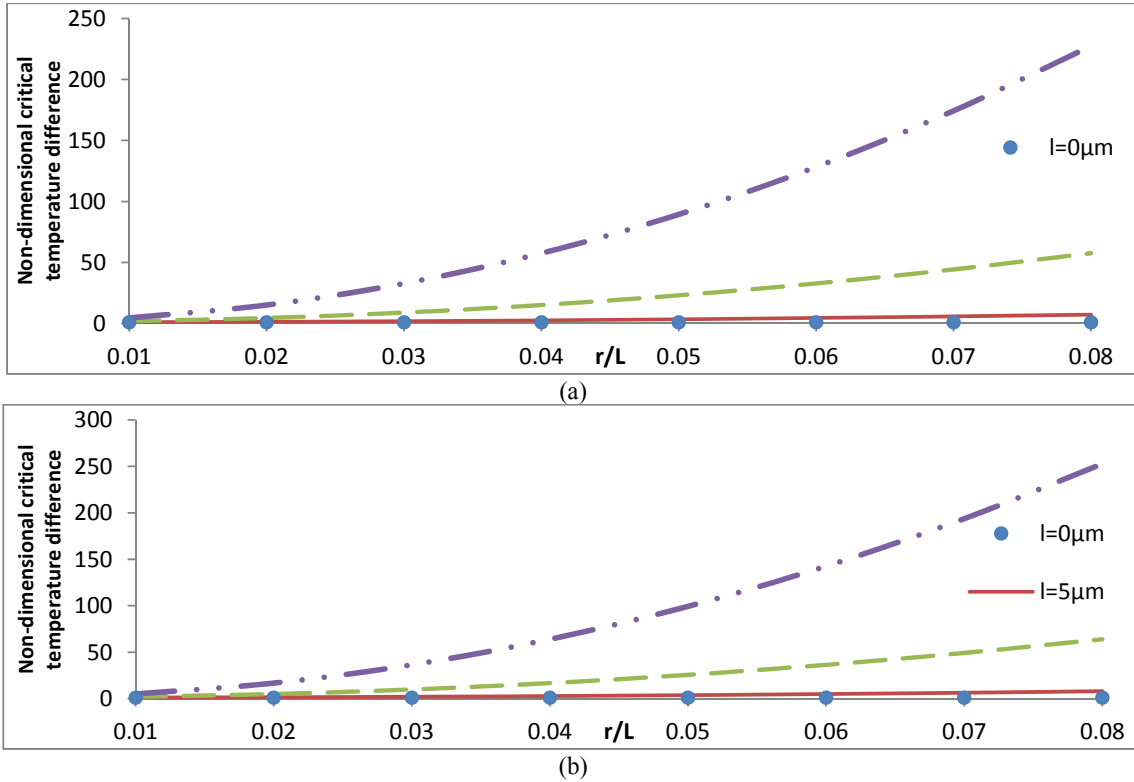


Fig. 8. Non-dimensional critical temperature difference a) hinged-hinged b) clamped-clamped by various theories ($L = 28 \mu m, r = 2 \mu m$)

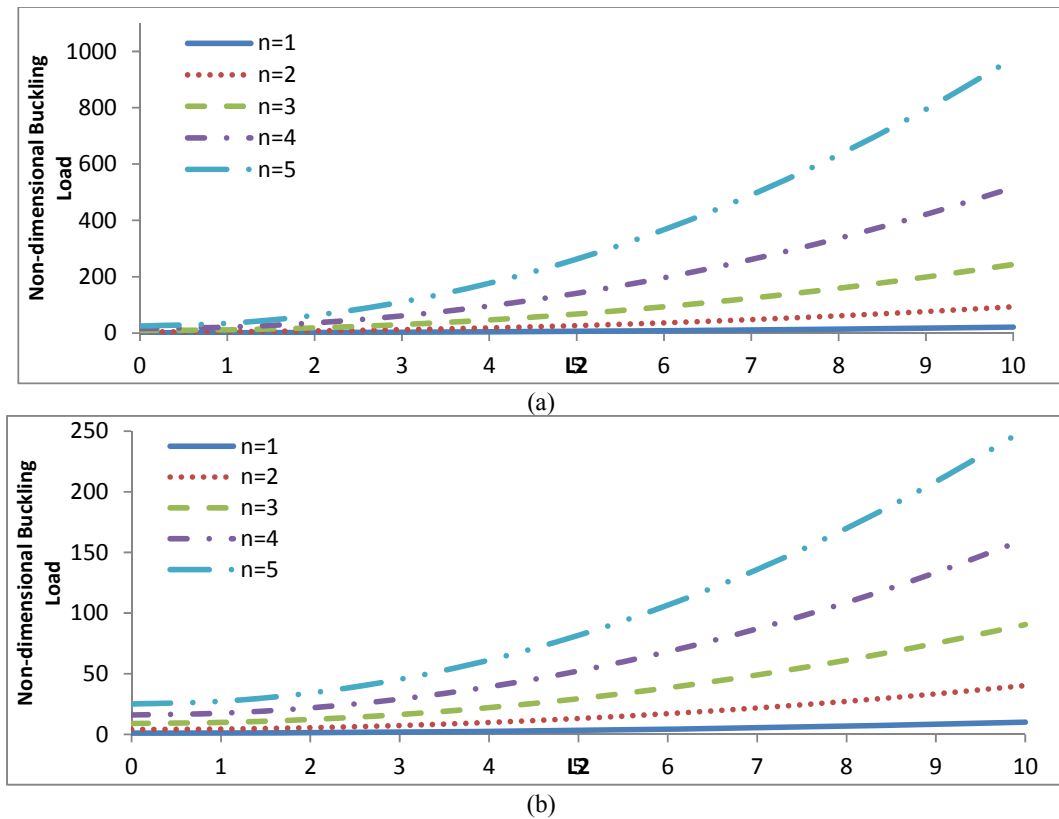


Fig. 9. Non-dimensional buckling load for a hinged-hinged microbeam with immovable boundary conditions for different modes a) MSGT b)MC ($L = 28 \mu m, r = 2 \mu m$)

5. CONCLUSION

This paper presented a new model for Euler-Bernoulli microbeam based on higher-order strain gradients for thermal buckling of microbeam, associated with small scale parameters. The results showed that the critical buckling load significantly increases as a result of considering the small scale parameters. This demonstrates that microbeam stiffness is larger due to small size effect. Poisson's effect seriously decreases the critical buckling load on the basis of modified strain gradient theory and must be considered, although it does not affect uniaxial critical buckling load on the basis of modified couple stress theory and classical theory. In the case of immovable axial boundary conditions, thermal loading could lead to buckling, while for the movable axial boundary conditions thermal loading cannot lead to buckling of microbeam but changes the compressive load induced in the microbeam. A higher critical temperature difference is observed for larger ratios of the radius of generation to length. Buckling load of microbeam decreases with increasing temperature difference.

REFERENCES

1. Mohammadi-Alasti, B., Ghader Rezazadeh, A.M., Borgheei, S. M. & Habibifar, R. (2011). On the mechanical behavior of a functionally graded micro-beam subjected to a thermal moment and nonlinear electrostatic pressure. *Compos. Struct.*, Vol. 93, pp. 1516-1525.
2. Yao, X. & Han, Q. (2007). The thermal effect on axially compressed buckling of a double-walled carbon nanotube. *Eur. J. Mech. A-Solid*, Vol. 26, pp. 298-312.
3. Wang, Y. Z., Li, F. & Kishimoto, M. K. (2010). Scale effects on thermal buckling properties of carbon nanotube. *Phys. Lett. A*, Vol. 374, pp. 4890-4893.
4. Ansari, R., Sahmani, S. & Rouhi, H. (2011). Axial buckling analysis of single-walled carbon nanotubes in thermal environments via the Rayleigh–Ritz technique. *Comp. Mater. Sci.*, Vol. 50, pp. 3050-3055.
5. Zhang, Y. Q., Liu, X. & Zhao, J. H. (2008). Influence of temperature change on column buckling of multiwall carbon nanotubes. *Phys. Lett. A*, Vol. 372, pp. 1676-1681.
6. Zhang, C. L. & Shen, H. (2006). Buckling and postbuckling analysis of single-walled carbon nanotubes in thermal environments via molecular dynamics simulation. *Carbon*, Vol. 44, pp. 2608-2616.
7. Zhang, C. L. & Shen, H. (2007). Thermal buckling of initially compressed single-walled carbon nanotubes by molecular dynamics simulation. *Carbon*, Vol. 45, pp. 2614-2620.
8. Ansari, R., Rouhi, H. & Sahmani, S. (2011). Thermal effect on axial buckling behavior of multi-walled carbon nanotubes based on nonlocal shell model. *Physica E*, Vol. 44, pp. 373-378.
9. Şimşek, M. & Yurtcu, H. H. (2012). Analytical solutions for bending and buckling of functionally graded nanobeams based on the nonlocal Timoshenko beam theory. *Compos. Struct.*, Vol. 97, pp. 378–386.
10. Lam, D.C.C., Yang, F., Chong, A.C.M., Wang, J. & Tong, P. (2003). Experiments and theory in strain gradient elasticity. *J. Mech. Phys. Solids*, Vol. 51, pp. 1477 – 1508.
11. Akgöz, B., & Civalek, Ö. (2011). Strain gradient elasticity and modified couple stress models for buckling analysis of axially loaded micro-scaled beams. *Int. J. Eng. Sci.*, Vol. 49, pp. 1268–1280.
12. He, Y., Brian, E. M. & Alan Overson, S., Nakamura, H., Christine, B. & Briscoe, J. F. (2000). Thermal characterization of an epoxy-based underfill material for flip chip packaging, *Therm. Acta.*, Vol. 357, pp. 1-8.
13. Yang, Q. & Lim, C.W. (2012). Thermal effects on buckling of shear deformable nanocolumns with von Kármán nonlinearity based on nonlocal stress theory. *Nonlinear Anal-Real*, Vol. 13, pp. 905–922.
14. Kong, S., Zhou, S., Nie, Z. & Wang, K. (2009). Static and dynamic analysis of micro beams based on strain gradient elasticity theory. *Int. J. Eng. Sci.*, Vol. 47, pp. 487–498.

15. Ma, H. M., Gao, X. L. & Reddy, J. N. (2008). A microstructure-dependent timoshenko beam model based on a modified couple stress theory. *J. Mechanics and Physics of Solids*, Vol. 56, pp. 3379-3391.
16. Kim, J. & Reddy, J. N. (2013). Analytical solutions for bending, vibration, and buckling of FGM plates using a couple stress-based third-order theory. *Compos. Struct.*, Vol. 103, p. 869.
17. Roque, C. M. C., Fidalgo, D. S., Ferreira, A. J. M. & Reddy, J. N. (2013). A study of a microstructure-dependent composite laminated Timoshenko beam using a modified couple stress theory and a meshless method. *Compos. Struct.*, Vol. 96, pp. 532-5.
18. Civalek, Ö. & Demir, C. (2011). Bending analysis of microtubules using nonlocal Euler-Bernoulli beam theory. *Appl. Math. Model.*, Vol. 35, pp. 2053-2067.
19. Akgöz, B. & Civalek, Ö. (2012). Analysis of micro-sized beams for various boundary conditions based on the strain gradient elasticity theory. *Arch. Appl. Mech.*, Vol. 82, pp. 423-443.
20. Ma, H. M., Gao, X. L. & Reddy, J. N. (2010). A non-classical reddy-levinson beam model based on a modified couple stress theory. *Int. J. Multiscale Comput. Eng.*, Vol. 8, pp. 167-180.
21. Liu, Y. & Reddy, J. N. (2011). A non-local curved beam model based on a modified couple stress theory. *Int. J. Struct. Stab. Dy.*, Vol. 11, No. 3, pp. 495-512.
22. Ma, H. M., Gao, X. L. & Reddy, J. N. (2011). A Non-classical Mindlin plate model based on a modified couple stress theory. *Acta Mech.*, Vol. 220, pp. 217-235.
23. Reddy, J. N. & Kim, J. (2012). A nonlinear modified couple stress-based third-order theory of functionally graded plates. *Compos. Struct.*, Vol. 94, pp. 1128-1143.
24. Reddy, J. N. & Arbind, A. (2012). Bending relationships between the modified couple stress-based functionally graded Timoshenko beams and homogeneous Bernoulli-Euler beam. *Annals Sol. Struct. Mech.*, Vol. 3, pp. 15-26.
25. Reddy, J. N. & Berry, J. (2012). Modified couple stress theory of axi-symmetric bending of functionally graded circular plates. *Compos. Struct.*, Vol. 94, pp. 3664-3668.
26. Roque, C. M. C., Fidalgo, D. S., Ferreira, A. J. M. & Reddy, J. N. (2013). A study of a microstructure-dependent composite laminated Timoshenko beam using a modified couple stress theory and a meshless method. *Compos. Struct.*, Vol. 96, pp. 532-537.
27. Şimşek, M. & Reddy, J. N. (2013). Bending and vibration of functionally graded microbeams using a new higher order beam theory and the modified couple stress theory. *Int. J. Eng. Sci.*, Vol. 64, pp. 37-53.
28. Şimşek, M. & Reddy, J. N. (2013). A unified higher order beam theory for buckling of a functionally graded microbeam embedded in elastic medium using modified couple stress theory. *Compos. Struct.*, Vol. 101, pp. 47-58.
29. Sinaie, A. & Abdi, B. (2003). On the optimal design of rib-stiffened columns using neural networks package (NETS). *Iranian Journal of Science & Technology, Transaction B, Engineering*, Vol. 28, No. 3, pp. 507-520.
30. Darvizeh, M. (2003). Buckling of fibrous composite cylindrical shells with non-constant radius subjected to different types of loading. *Iranian Journal of Science & Technology, Transaction B, Engineering*, Vol. 28, No. 3, pp. 535-550.
31. Motallebi hasankola, S. S., Goshtasbi rad, E. & Abouali, O. (2012) Experimental investigation of the airflow around supported and surface mounted low rise rural buildings. *Iranian Journal of Science & Technology, Transactions of Mechanical Engineering*, Vol. 36, pp. 143-153.